Rno-miR-199a-3p targets Nedd4 to promote sensitization of ST36 acupoints via mast cell activation in a rat model of knee osteoarthritis

Wenchuan Qi
Chengdu University of TCM: Chengdu University of Traditional Chinese Medicine
Baitong Liu
Chengdu University of TCM: Chengdu University of Traditional Chinese Medicine
Yilu Jiang
Chengdu University of TCM: Chengdu University of Traditional Chinese Medicine
Xinye Luo
Chengdu University of TCM: Chengdu University of Traditional Chinese Medicine
Zhiwei Li
Chengdu University of TCM: Chengdu University of Traditional Chinese Medicine
Qianhua Zheng
Chengdu University of TCM: Chengdu University of Traditional Chinese Medicine
Fanrong Liang
Chengdu University of TCM: Chengdu University of Traditional Chinese Medicine
Ding-jun CAI (djcai@cdutcm.edu.cn)
Chengdu University of Traditional Chinese Medicine https://orcid.org/0000-0002-4298-9940

Research

Keywords: knee osteoarthritis、acupoint sensitization、ST36 acupoint、 rno-miR-199a-3p、neural precursor cell expressed developmentally down-regulated 4 (Nedd4)、mast cell

Posted Date: October 12th, 2021

DOI: https://doi.org/10.21203/rs.3.rs-929701/v1

Abstract

Selecting routine points on related meridians is widely accepted as the foundational principle of acupuncture. When the body is suffering disease or injury, corresponding acupoints are thought to be activated and manifest in several sensitized forms. Sensitized acupoints hold high clinical value as a reflection of disease activity on the body surface. Mast cells have been implicated in the process of acupoint sensitization but the underlying regulatory mechanisms remain unclear. In the present study, we evaluated ST36 as a sensitized acupoint in the monosodium iodoacetate-induced knee osteoarthritis rat model. We first confirmed sensitization at the ST36 acupoint through decreases in the acupoint mechanical pain threshold and instructively found an accompanying increase in skin mast cell degranulation. Thereafter, we used highthroughput RNA sequencing to reveal potential molecular mechanisms of acupoint sensitization. We showed that rno-miR-199a-3p was highly expressed in the sensitized ST36 acupoint and its expression was associated with mast cells. Functional experiments revealed that overexpression of rno-miR-199a-3p increased mast cell histamine release whereas inhibition of rno-miR-199a-3p decreased histamine release. Mechanistically, we established rno-miR-199a-3p acted to inhibit neural precursor cell expressed developmentally down-regulated 4 (Nedd4) protein expression through miRNA-mediated targeting of the 3’-UTR of Nedd4 mRNA. Moreover, we found ectopic expression of Nedd4 antagonized histamine release in mast cells and blocked the actions of rno-miR-199a-3p overexpression. Thus, our study establishes that mast cells participate in the process of acupoint sensitization, and further reveals a novel miRNA-based mechanism which is crucial for further understanding of acupoint sensitization and acupuncture applications.

1. Introduction

Acupuncture was first introduced to the Western world in the 20th century. Indeed, acupuncture is now recognized as an effective treatment and has become one of the most common auxiliary and alternative therapies worldwide [1]. The specific effector sites for needle insertion in acupuncture are known as acupoints, and these are widely considered the core focus of acupuncture research[2]. Previous studies have shown that acupoints are not fixed, rather their position and function can change dynamically according to physiological and pathological conditions[3]. In this process, the term acupoint sensitization refers to the dynamic transformation of acupoints from "silent state" (health) to "active state" (disease)[4, 5]. When the body suffers disease or injury, the corresponding acupoints will be activated and appear in several sensitization forms, including the expansion of neuron receptive field, pain sensitization and heat sensitization[6, 7]. This phenomenon may gradually disappear with disease recovery. Acupoint sensitization significantly affects the receptive field size and sensitivity of acupoints, thus enhancing their therapeutic functions, including receiving stimulation and regulating body functions[8]. In modern acupuncture and moxibustion clinical practice, the correct application of acupuncture treatments can guarantee the efficacy of disease treatment[9–11]. Therefore, selection of the specific sites representing sensitized acupoints is of great significance for the prescription and clinical efficacy of acupuncture.

The occurrence and development of acupoint sensitization is closely related to the microphysical environment and chemical changes of local tissues[4, 12]. Increasing research efforts have broadly contributed to a deepening understanding of acupoints, with the realization that acupoints are not single static points, but change according to the physiological and pathological state of the body[5]. For example, it was found that when acute gastric mucosal injury leads to a neuronal inflammatory response, there were more sensitization points in a relatively concentrated area of the body surface, and these sensitization points have a greater correlation with acupoints[13, 14]. Notably, mast cells are important immune cells and widely considered as potential effector cells in acupuncture treatment[15, 16] and appear to be one of the key signal amplification factors in acupuncture effects[16]. In support of this concept, one pilot study found that the density of mast cells from the ST36 acupoint in rats was higher than a nearby sham point[17]. At the same time, mast cells numbers along with their degranulation rate are one of the important indicators of acupoint sensitization [4, 18]. Therefore, it is necessary to clarify the structural changes and functional characteristics of mast cells at acupoints to improve acupuncture treatments and to better understand the connotation of acupoints.

The local microenvironment has also been identified as an important acupuncture target and is closely related to the effects of acupuncture [4]. Previous studies mainly focused on the effects of acupuncture on chemical mediators such as histamine, 5-HT and trypsin, and their regulatory mechanisms. However, other potential regulatory mechanisms during acupoint sensitization such as those involving microRNAs (miRNAs) have been ignored to some extent. At present, most related studies have focused on the regulatory role of miRNAs in acupuncture treatment [19, 20], but whether miRNAs are involved in the regulation of acupoint sensitization is still unclear.

Knee osteoarthritis (KOA), also known as knee degenerative osteoarthritis, is a chronic and degenerative disease characterized by the degeneration, destruction, and hyperplasia of articular cartilage. In traditional Chinese medicine, KOA belongs to the category of bone arthralgia. Animal models of KOA have been commonly used in experimental acupuncture studies and have proved useful in the study of acupoint sensitization. In the context of this study, KOA model animals have been used to study the relationship between acupoint sensitization and the characteristics of mast cells in sensitized acupoints. For instance, one study demonstrated that elevated GlyT2 expression was a crucial mediator of ST35 acupoint sensitization in KOA rats[21], while early laser moxibustion significantly reversed monosodium iodoacetate-induced (MIA)-induced mechanical hyperalgesia[22].

Based on the limited information currently available, our study aimed to explore the contribution of miRNAs to the acupoint sensitization phenomenon in a rat model of KOA. We used a von Frey electronic pain meter and infrared thermal imager to detect the mechanical pain threshold and temperature of acupoints near the knee joint in KOA model rats. Differentially expressed miRNAs were then identified through high-throughput sequencing after extracting miRNAs from subcutaneous connective tissue of the sensitized acupoints. In parallel, we also determined the differential expression of miRNAs in mast cells extracted from the sensitized acupoints and assessed their function in regulating degranulation. Together

this information provides a valuable reference for explaining the regulatory mechanisms governing acupoint sensitization.

2. Materials And Methods

Animals and ethics

Male Sprague–Dawley rats (350–450 g, SCXK (Chuan) 2015-030; Dashuo Co.Ltd. Chengdu, China) were housed under controlled conditions (12:12 h light: dark cycle, 22–24ºC, 40–60% relative humidity) with food and water ad libitum. All experimental procedures were approved by the Chengdu University of Traditional Chinese Medicine Animal Welfare and Ethics Committee and conformed to the standards of the International Council for Laboratory Animal Science.

Cell culture

Rat skin mast cells were purchased from Procell Life Science Technology Co. Ltd. (Wuhan, China) and the human embryonic kidney cell line (HEK-293) was obtained from Cell Bank of Chinese Academy of Sciences (Shanghai, China). Cells were cultured in DMEM (Gibco, USA) containing 10% fetal bovine serum, 100 U/mL penicillin, and 100 mg/mL streptomycin at 37°C in a humidified incubator (Panasonic, Japan) with 5% CO_2.

MIA-induced KOA model

Rats (n = 68) were randomly assigned to two groups comprising normal saline (NS) and model groups (KOA). The NS group received a 50 μL injection of 0.9% saline into the left knee whereas rats in the KOA group were anesthetized with isoflurane (RWD, Shenzhen, China) and subject to a single intra-articular injection of MIA (3 mg/50μL; Sigma,USA) dissolved in 0.9% saline in the left knee joint through the infrapatellar ligament, as previously described[23].

Model evaluation

We first compared the diameter of left knee joint of all rat before and after treatment. After detecting the mechanical pain threshold, selected rats from the NS and KOA groups were used for pathological examination of knee cartilage. Briefly, the rats were sacrificed and the joints exposed before separating the upper and lower articular surfaces, stripping, and visually observing the muscle and ligament tissues. Thereafter, the bone and cartilage tissues 1 cm above the tibial plateau were fixed in 4% formaldehyde solution and subjected to paraffin embedding and sectioning before conducting H&E staining. The articular cartilage pathology was then observed and imaged with a light microscope (Leica, Milan, Italy).

Left knee joint diameter measurements

The transverse diameters of the knee were measured at days 0 and 14 with a slide caliper (Mitutoyo, Japan) to measure the horizontal distance between the highest left and right points of the knee joints,

respectively, when flexed at 90°. Each knee was measured three times, and the mean values recorded.

Measurement of acupoint sensitization

Acupoint mechanical thresholds were determined by measuring the incidence of foot withdrawal in response to mechanical indentation of ST36. An electronic Von Frey algesimeter (IITC Life Science Inc, America) was used to detect the mechanical pain threshold of the ST36 acupoints in NS and KOA rats prior to treatment and after 14 days. The mechanical pain threshold was detected average for three times and the change rate of mechanical pain threshold was calculated as: (mean value after model-value before model)/(mean value before model).

Histologic examination of ST36 acupoint skin

Skin tissues from the ST36 acupoint were fixed with 10% formalin in PBS and then embedded in paraffin. Skin sections with a thickness of 5 mm was prepared and stained with toluidine blue before examination using light microscopy (Leica, Milan, Italy).

RNA extraction and miRNA sequencing

Tissue samples were flash frozen in liquid nitrogen and stored at − 80°C until nucleic acid extraction. In total, 200 mg of fresh frozen tissues were used to isolate total RNA with the mirVana™ miRNA Isolation Kit (Thermo Fisher Scientific, Waltham, MA, USA). A NanoDrop spectrophotometer (Thermo) was used to estimate total RNA concentration while an Agilent 2100 Bioanalyzer (Agilent Technologies, Inc., Santa Clara, CA, USA) was used to measure the quantity and purity of small RNAs. Small RNA libraries were constructed using the TruSeq Small RNA Sample Preparation kit (Illumina, San Diego, CA) according to the manufacturer's protocols. Briefly, small RNA samples were ligated with 5’ and 3’ adapters, followed by reverse transcription-PCR (RT-PCR) for cDNA library construction and incorporation of index tags. The cDNA library fragments were purified separated on TBE PAGE gels and the fraction containing miRNA inserts were isolated. The cDNA library samples were pooled in equimolar amounts and used for cluster generation and sequence analysis in a single lane on an Illumina HiSeq2000 by Shanghai Biotechnology Corporation.

Bioinformatics analysis

Raw FASTQ sequences were generated and demultiplexed using the Illumina CASAVA v1.8 pipeline. Per base sequence quality was then assessed using the FastQC toolkit (http://www.bioinformatics.babraham.ac.uk/projects/fastqc). Briefly, the 3’ adapter sequences were trimmed, the read size filtered (16–35nt), unique reads counted and low abundance reads (< 10 reads) discarded. Unique sequence reads were then aligned to the rat genome and miRBase_v16 using the miRanalyzer web server tool (http://bioinfo2.ugr.es/miRanalyzer/miRanalyzer.php). MiRanda database was applied to predict the targeted binding of the differential miRNA and the 3'UTR of mRNA obtained in the previous step. The address of the miRanda database is http://www.microma.org/. The main functions of the predicted target genes regulated by differentially expressed miRNAs were determined

using KEGG functional classifications by database for annotation, visualization, and integrated discovery (DAVID 6.8). The address of KEGG database is http://www.genome.jp/kegg/.

Real-time quantitative PCR (RT-qPCR)

RNA was extracted using TRIzol® reagent (Invitrogen; Thermo Fisher Scientific, USA) and subsequently treated with DNase I (Thermo Fisher Scientific, USA). Primers were designed using Primer Express 3.0.1 and synthesized by Sangon Biotech (Shanghai) Co. Ltd. First-strand cDNA synthesis was carried out by using a Reverse Transcription System Kit according to the manufacturer's instructions (#11801-025, OriGene Technologies, USA). The indicated miRNAs were amplified from cDNA with the following specific primers:

rno-miR-199a-3p GACAGTAGTCTGCACATTGGTTAA

rno-miR-199a-5p CCCAGTGTTCAGACTACCTGTT

rno-miR-214-3p ACAGCAGGCACAGACAGG

rno-miR-205 TCCTTCATTCCACCGGAG

rno-miR-543-3p AAACATTCGCGGTGCAC

U6 TTCGTGAAGCGTTCCATATTTT

To detect Nedd4 mRNA expression, the primers used were as follows:

Nedd4 forward CGGAGGACGAGGTATGGGAG

Nedd4 reverse AAGGACTCCACTCATCGGGT

Actin forward CACCCGCGAGTACAACCTTC

Actin reverse CCCATACCCACCATCACACC

U6 was applied as an internal control for miR-199a-3p while actin was used for assays measuring Nedd4. RT-qPCR reactions were performed and analyzed with a

QuantStudio Dx Real-Time Instrument (Thermo Fisher Scientific, USA) and QuantStudio™ Design & Analysis software using the following reaction conditions: 50°C,2 min; 95°C 10 min(95°C, 15 s; 60°C, 1 min) x 40 cycles. Expression levels were calculated using the $2^{-\Delta\Delta}$ CT data analysis method.

Isolation and culture of ST36 skin mast cells

Skin mast cells were isolated according to a previous report using aseptic techniques [24]. Briefly, the ST36 acupoint skin was cut into comb-like pieces and transferred to medium containing Dulbecco's

Phosphate-Buffered Saline (DPBS) with Ca^{2+} and Mg^{2+} (Beyotime) containing 2.4 U/ml Dispase Type II (Solarbio) and incubated overnight at 4°C. The next day, the epidermis was removed from the dermis with fine forceps. The homogenized dermis was then transferred for secondary digestion for 60 min at 37°C with DPBS containing collagenase, hyaluronidase, and DNase (all from Solarbio). The resulting suspension was filtered through a mesh sieve and centrifuged at 400 g for 10 min at 4 °C. Cell pellets were then resuspended in cold DPBS and after further centrifugation, resuspended in MACS buffer (Thermo Fisher Scientific, USA) and filtered sequentially through cell strainers. After centrifugation, the cells were suspended in 1 ml of cytokine free MC culture medium (Basal Iscove's medium (Gibco) with 10% fetal bovine serum (HyClone), penicillin–streptomycin (HyClone), nonessential amino acids (Procell, Wuhan, China), and α-monothioglycerol (RHAMN, Shanghai, China) and cultured at 37°C in a cell culture incubator (Thermo) for 24 h. Mast cells were identified by toluidine blue staining

MiRNA / plasmid transfection

Rat skin mast cells and HEK-293 cells were used in transfection experiments as indicated. Control rno-miRNA (rno-miRNA-NC), rno-mir-199a-3p mimic and rno-mir-199a-3p inhibitors were purchased from RiboBio (Guangzhou, China). Nedd4 related plasmids were synthesis by TsingKe Biological Technology (Chengdu, China). For miRNA / plasmid transfection, cells were seeded in six-well dishes at a density of 2.0×10^5 cells per well 24 h prior to transfection. Thereafter, transfections were performed with Lipofectamine 2000 (Invitrogen, Carlsbad, Calif) and the cells harvested 48 h later for analysis.

Western blotting

Whole cell lysates were extracted using NP-40 Lysis buffer (Beyotime, Shanghai, China) and protein concentrations quantified using a BCA protein assay kit (Beyotime Biotechnology, Shanghai, China). Western blotting was performed according to standard procedures using rabbit polyclonal anti-Nedd4 antibody, mouse monoclonal anti-flag antibody and rabbit monoclonal anti-actin antibody along with appropriate horseradish peroxidase (HRP)conjugated secondary antibodies (Proteintech, Chicago, USA). Actin protein levels served as a loading control.

Fluorescence in situ hybridization

RNA fluorescence in situ hybridization (FISH) was performed as described previously on sections of paraffin-embedded tissues [25]. Briefly, sections were dewaxed at 62°C for 2 hours and then rehydrated in DEPC dilution (Amresco,USA). The sections were then boiled for 10–15 minutes, treated with proteinase K (20 ug/ml□Servicebio) and then washed 3 times in PBS. Thereafter, the sections were incubated for 1 h at 37°C in pre-hybridization solution (Servicebio) before hybridization overnight with miRNA probes in hybridization solution. The sections were then washed with different concentrations of SSC solution (Servicebio). Cell nuclei were counterstained with DAPI (Servicebio) before mounting and observation using an epifluorescence microscope (Nikon Eclipse CI, Nikon, Japan). A Cy3-labelled rno-miR-199a-3p probe purchased from Shanghai Sinomics Corporation was used to detect miR-199a-3p (CACAAATTCGGTTCTACAGGGTA) [18]. Cyanine 3 was detected at excitation wavelengths of 510–560

nm and emission wavelength of 590 nm while DAPI was detected by excitation wavelengths of 330–380 nm and emission wavelength of 420 nm.

Histamine release assay

Rat mast cells were treated with 50 μm substance P (SP) (Selleck,Shanghai, China) for 30 min before collected supernatants to measure the amounts of secreted histamine using a histamine ELISA kit according to the manufacturer's instructions (Elabscience Biotechnology Co. Ltd, Wuhan, China). Values were measured using a spectrophotometer (Epoch, BioTECH, USA) and data expressed as nanograms per milliliter of histamine.

Statistical analysis

All statistical analyses were performed using SPSS 19.0 software (Chicago, IL, USA). Statistical tests ANOVA and a t-test were used in results as described. When ANOVA was used, a Tukey post hoc test was performed for means comparison. Two-sided $P < 0.05$ were considered significant.

3. Results

1. Construction and evaluation of the KOA rat model

We constructed a KOA model by injecting monosodium iodoacetate into the left knee joint cavity of rats and compared this to a control group injected with the same volume of normal saline (NS). After 14 days we observed a series of pathological changes in rat synovial tissues in the KOA rats including roughness in the surface of articular cartilage, local defects and increases or decreases in joint fluid along with obvious osteophytes found around the cartilage. In comparison, no significant pathological changes were evident in the NS group (Fig. 1A). In parallel, we assessed the pathological changes by examining H&E stained synovial sections. As anticipated, there were no obvious changes in the NS group tissues whereas a number of pathological changes were evident in the KOA group including articular cartilage defects, fibrous tissue proliferation and chondrocyte necrosis (Fig. 1B). Additionally, from the functional viewpoint, the treated leg in the KOA group appeared limp and the rats were reluctant to exercise the affected limb. Moreover, KOA group rats showed higher scores in pain stimulation response, gait, joint activity, and joint swelling than the NS group. Vernier caliper measurements also revealed that the diameter of left knee joints before and after treatment was increased in both NS and KOA groups (Fig. 1C). However, the joint diameter increases in the KOA group were significantly more than the NS group ($P < 0.05$), whereas the NS group changes were not statistically significant ($P < 0.05$). Together these data indicate that injection of MIA induced rat KOA-related cartilage damage, thus establishing the suitability of the model to study KOA.

2. Acupoint Sensitization Detection And Determination Of Sensitization State

As a frequently used acupoint for acupuncture treatments involving KOA, we selected ST36 as the acupoint for our sensitization studies. A von Frey electronic pain meter was used to detect the mechanical pain threshold of the relevant acupoints of each rat before and after the model treatments. The calculated changes in pain threshold rates were used as the criterion for determining sensitization acupoints. As shown in Fig. 2A, there was no significant change in the ST36 pain threshold in the NS group, but notably the pain threshold in the KOA group was significantly decreased. This proposes that the ST36 acupoints in the KOA group were sensitized.

As described in the introduction, mast cell accumulation and degranulation are important signs of acupoint sensitization [4]. Interestingly, we observed a non-significant trend that the total number of mast cells in the ST36 acupoint was increased in the KOA group compared to the NS group ($P > 0.05$; Fig. 2B). Since it is known that mast cells are concentrated in the ST36 acupoint [17] this fact may have affected the level of significance. Nonetheless, the levels of mast cell degranulation in the sensitized ST36 acupoints were significantly higher in KOA compared to the NS treatments, along with their degranulation rate ($P < 0.05$; Fig. 2C and 2D). Phenotypic examination using toluidine blue staining clearly revealed more degranulated mast cells in the skin at the ST36 acupoint in the KOA group compared to the NS group (Fig. 2E and 2F). Together these data indicate that ST36 acupoint sensitization in KOA was associated with increased mast cell degranulation.

3. **RNA-seq reveals differentially expressed miRNAs in the sensitized ST36 acupoint**

We hypothesized that miRNAs would be likely mediators of acupoint sensitization. To test this, we employed transcriptome sequencing to identify differentially expressed miRNAs in skin tissues between sensitized ST36 acupoints in the NS and KOA groups. This approach identified a total of 8 miRNAs whose expression was significantly different between the KOA and NS groups. Of these, 1 miRNA was down-regulated, and 7 miRNAs were up-regulated in the KOA group. To verify the transcriptomic data, we randomly selected a subset of samples (n = 3/each group) and used RT-qPCR (n = 6/each group) to measure 4 of the differentially expressed miRNAs identified in the RNA-seq analysis, specifically rno-miR-199a-3p,rno-miR-199a-5p□rno-miR-205□rno-miR-214-3p, and rno-miR-543-3p. Using U6 snRNA as a reference gene we found that there was a similar tendency between the RNA-seq and RT-qPCR data for all 4 miRNAs, however, only rno-miR-205 and rno-miR-199a-3p were significantly changed ($P < 0.05$; Fig. 3A). Notably, rno-miR-199a-3p had been previously implicated in the regulation of mast cell function [28].

Next to investigate potential pathways involved in KOA modelling, we utilized the Kyoto Encyclopedia of Genes and Genomes (KEGG) pathway analysis from DAVID. The predicted actions of the differentially expressed miRNAs included effects on genes involved in mast cell activation pathways such as the Fc epsilon RI signaling [26, 27] (Fig. 3B). This prediction together with our findings led us to focus on the potential role of rno-miR-199a-3p in acupoint sensitization.

4. High expression of rno-miR-199a-3p in the ST36 acupoint contributes to mast cell activation

Our preceding results established that rno-miR-199a-3p was highly expressed in the ST36 acupoint skin of the KOA group rats. In order to determine whether the increased expression was associated with mast cells, we utilized fluorescence in situ hybridization (FISH) to reveal the cellular location of rno-miR-199a-3p. We observed that rno-miR-199a-3p fluorescence signals were noticeably higher in mast cells in the KOA group skin compared to the NS group (Fig. 4A), suggesting increased rno-miR-199a-3p levels in mast cells in the KOA group. To confirm this notion, we extracted mast cells from ST36 acupoint skin from the KOA and NS groups and measured the relative levels of rno-miR-199a-3p using RT-qPCR. Indeed, these results confirmed that the expression level of rno-miR-199a-3p in KOA rats ST36 acupoint mast cells was significantly increased (Fig. 4B).

To further validate the role of rno-miR-199a-3p in mast cells, we transfected rno-miR-199a-3p inhibitors or NC controls into cultured mast cells. The results showed rno-miR-199a-3p expression was significantly reduced in inhibitor-treated mast cells compared to mock or NC-treated cells (Fig. 4C). Instructively, inhibition of rno-miR-199a-3p levels resulted in significantly decreased histamine release from mast cells after treatment with substance P (SP) (Fig. 4E), which is a commonly used technique to stimulate mast cells in the field of acupuncture research[29, 30]. Alternatively, rno-miR-199a-3p mimics were also transfected into rat skin mast cells to overexpress rno-miR-199a-3p. As anticipated, after transfection the measured levels of rno-miR-199a were significantly increased (Fig. 4D) and such overexpression promoted increased HA release from mast cells after treatment with SP (Fig. 4E). Taken together, these data indicate that upregulation of rno-miR-199a-3p significantly increases histamine release in mast cells, proposing a functional link between rno-miR-199a-3p and the activation of mast cells in the ST36 acupoint in KOA.

5. Mast cell activation through rno-miR-199a-3p results from inhibition of Nedd4

MicroRNAs function as post-transcriptional gene regulators by targeting specific mRNAs to cause downstream effects on the levels of their corresponding proteins. We next used the TargetScan database to identify the likely targets of rno-miR-199a-3p in mast cells. Of the candidate genes identified, we selected Nedd4 for further investigation because of its known functions related to mast cell activation[31]. As shown in Fig. 5A, the potential miRNA binding site was located at bases 366 to 373 in the Nedd4 3’ UTR. On this basis, we constructed pmiR-GLO luciferase reporter vectors containing the 3’-UTR of the Nedd4 mRNA with the predicted rno-miR-199-3p binding sequence intact (wild-type) or mutated as illustrated. Then to test whether Nedd4 was directly regulated by rno-miR-199a-3p, we transfected the wild-type or mutant vectors in combination with either rno-miR-199a-3p mimics or the control NC mimics into HEK-293 cells. We found that the introduction of the rno-miR-199a-3p mimics inhibited the luciferase reporter activity of the wild-type but not the mutant vector (Fig. 5B), indicating that rno-miR-199a-3p targets Nedd4 mRNA though the identified binding site. Substantiating this result, transfecting cultured mast cells with rno-miR-199a-3p mimics resulted in significant decreases in the levels of Nedd4 mRNA (Fig. 5C) and protein (Fig. D). These results indicate that rno-miR-199a-3p can directly inhibit Nedd4 expression by targeting Nedd4 mRNA.

6. Rno-mir-199a-3p Promotes Mast Cell Activation Via Nedd4

Lastly, we sought to verify whether the functional effects of rno-miR-199a-3p on mast cell activation were mediated by targeting of Nedd4. Towards this we performed rescue assays where the reduced levels of Nedd4 resulting from rno-miR-199a-3p inhibition were reversed by ectopic expression of Flag-tagged Nedd4. Notably, the overexpression of Flag-Nedd4 alone in cultured mast cells resulted in significant reductions in HA release. In contrast, simultaneous transfection of Flag-Nedd4 with rno-miR-199a-3p mimics predominantly blocked increases in HA release (Fig. 6A). Taken together, these data indicate that rno-miR-199a-3p promotes mast cell activation by regulating Nedd4 expression.

4. Discussion

Acupuncture has been used as an effective alternative therapy for knee arthritis worldwide. A variety of evidence shows that acupuncture can reduce the pain associated with knee osteoarthritis, improve knee joint function, and often cooperates with other drugs [32, 33]. According to traditional Chinese medicine, acupoints used in clinical practice usually represent the reflex points of specific diseases (i.e., sensitized acupoints)[3]. Extensive clinical research on acupuncture has made clear the regularity of acupoint selection in KOA treatment, and provided important insights for acupoint selection. On this basis, knee osteoarthritis represents an ideal condition to study the process of acupoint sensitization.

Acupuncture treatments for knee osteoarthritis are typically prescribed through several acupoints around the knee such as GB34 and ST36[34]. For our study, we selected ST36 as the target acupoint for experimental analysis and found that the pain threshold of ST36 changed after KOA modeling in rats. Many studies on acupoint sensitization have shown this process is closely related to mast cells[4, 14, 21]. For example, in a gastrointestinal mucosa chemical injury model the Evans blue (EB) exudation points in corresponding acupoint skin tissues increased, along with mast cell aggregation and degranulation rates. Our study provides additional support for this concept where we found definitive evidence showing increased mast cell degranulation rates in ST36 sensitized acupoints after KOA modeling.

Mast cells are important immune cells [35, 36] which are mainly derived from bone marrow precursor cells but circulate in the blood to reach target tissues where they differentiate and mature [37, 38]. For example, mature mast cells are observed in the skin, nasal cavity and intestinal mucosa[37, 39]. Mast cells respond to a variety of physical and chemical stimuli, such as viral infections, bacterial invasion, mechanical and heat stimulation, causing them to release cytokines and chemokines[40, 41]. Additionally, mast cell activation also results in the release active substances such as histamine (HA), tryptase and 5-hydroxytryptamine (5-HT)[42, 43]. Through exocytosis, these substances may promote local skin allergic reactions, from which pain sensitization occurs. The sensitization of acupoints is related to the aggregation and degranulation rate of mast cells with the release of trypsin, 5-HT and HA likely playing a role [44]. Moreover, others have provided clear evidence that neuropeptide release from mast cells in the local skin microenvironment is also important for acupoint sensitization. Substance P is

a prokinetic brain gut peptide widely distributed in nervous system and gastrointestinal nervous system [45–47] and represents a signaling substance recognized by the nervous, endocrine, and immune systems. In mast cells, SP occurs in the context of a positive feedback loop where SP promotes mast cell degranulation, which in turn, release substances including SP to promote further mast cell degranulation in a time and dose-dependent manner. SP is also is of the substances that cause the meridian effect which appears to require the cooperation of mast cells[30]. Consistently, we found in our study that mast cells within the sensitized ST36 acupoints showed increased activation and degranulation. Further mechanistic studies also revealed that expression level of rno-miR-199a-3p in the ST36 skin tissue was significantly increased and specifically associated with mast cells. We also modelled mast cell activation in vitro using by treating cells with SP and assessing degranulation through the release of HA. Using rno-miR-199a-3p inhibitors and mimics, the key finding was made that the expression levels of rno-miR-199a-3p positively influenced mast cell degranulation rates. Furthermore, we showed this effect on mast cell degranulation and histamine release was attributed to rno-miR-199a-3p targeting of Nedd4 mRNA which inhibited Nedd4 protein expression. Therefore, the rno-miR-199a-3p-Nedd4 axis may be one of the key regulatory processes involved in acupoint sensitization.

In summary, our study proposes for the first time that a miRNA-mediated regulatory mechanism is responsible for regulating acupoint sensitization. However, there are some limitations of the study that must be acknowledged. We judged the occurrence and degree of sensitization by the decrease of acupoint mechanical pain threshold and the change rate. However, whether the difference of miRNA expression can be used as the standard to judge acupoint sensitization remains to be answered. Nor did we evaluate all other miRNAs identified by this analysis. Thus in order to determine the diagnostic criteria of sensitization in animal experiments, it will be necessary to further carry out larger sampling and adopt additional research methods. Furthermore, while our research suggests that miR-199a-3p was associated with mast cells and promotes mast cell degranulation, its origin is still unknown. It has been reported that miR-199a-3p also exists in exosomes[48–50] and therefore miR-199a-3p could conceivably be transported to the ST36 acupoint by exosomes. For example, an attractive hypothesis is that the increased rno-miR-199a-3p originates from secretions in the injured knee joint and is transported via exosomes to mast cells in the ST36 skin acupoint. However, this hypothesis needs further research.

5. Collusion

In this study,We found that ST36 acupoints in the KOA group were sensitized. Rno-miR-199a-3p was highly expressed in the sensitized ST36 acupoint and its expression was associated with mast cells. Overexpression of rno-miR-199a-3p increased mast cell histamine. Mechanism, rno-miR-199a-3p may promotes mast cell activation by regulating Nedd4 expression. Together, our study establishes that mast cells participate in the process of acupoint sensitization, and further reveals the rno-miR-199a-3p-Nedd4 axis may be one of the key regulatory processes involved in acupoint sensitization.

Abbreviations

KOA Knee osteoarthritis

Nedd4 neural precursor cell expressed developmentally down-regulated 4

miRNA microRNAs

MIA monosodium iodoacetate

MC mast cell

HA histamine

5-HT 5-hydroxytryptamine

H&E hematoxylin-eosin staining

PCR Polymerase Chain Reaction

RT-PCR reverse transcription-PCR

KEGG Kyoto Encyclopedia of Genes and Genomes

DPBS Dulbecco's Phosphate-Buffered Saline

HRP horseradish peroxidase

FISH RNA fluorescence in situ hybridization

SP substance P

NS normal saline

WT wild-type

Declarations

Ethics approval and consent to participate

This study was approved by the Committee on Ethical Use of Animals of Chengdu University of Traditional Chinese Medicine.

Consent for publication

Not applicable.

Availability of data and materials

The datasets used and/or analysed during the current study are available from the corresponding author on reasonable request.

Conflicts of Interest

The authors declare no conflicts of interest.

Foundation Project

This work was supported by the National Natural Science Foundation of China (81774400),Sichuan Province Science and Technology Plan Project (2019YJ0330) and China Postdoctoral Science Foundation (No. 2020M683642XB).

Author Contributions

D-JC, F-RL and W-CQ conceived and designed the experiments. W-CQ and B-TL did most of the experiments and analyzed the data. Y-LJ helped with RT-qPCR experiments. X-YL helped with the western blot experiments. B-TL Y-LJ X-YL and Z-WL helped with the rat model and measurement of acupoint sensitization. Q-HZ helped with the data collection. W-CQ wrote the manuscript. All authors reviewed and revised this manuscript and reviewed the final version of the manuscript.

Acknowledgements

The authors would like to express their gratitude to EditSprings (https://www.editsprings.com/) for the expert linguistic services provided.

References

1. Kaptchuk TJ. Acupuncture: theory, efficacy, and practice. Ann Intern Med. 2002;136(5):374–83.
2. Hwang YC. Anatomy and classification of acupoints. Probl Vet Med. 1992;4(1):12–5.
3. Li F, He T, Xu Q,et al. What is the Acupoint? A preliminary review of Acupoints. Pain Med. 2015;16(10):1905–15.
4. Ding N, Jiang J, Qin P, et al. Mast cells are important regulator of acupoint sensitization via the secretion of tryptase, 5-hydroxytryptamine, and histamine. PLoS One. 2018;13(3):e0194022.
5. Zhu B. The plasticity of acupoint. Zhongguo Zhen Jiu. 2015;35(11):1203–8.
6. Yu X. Zhu B, Lin Z, et al. Acupoint Sensitization, Acupuncture Analgesia, Acupuncture on Visceral Functional Disorders, and Its Mechanism. Evid Based Complement Alternat Med. 2015;2015:171759.
7. Chen RX, Kang MF, et al. Clinical application of acupoint heat-sensitization. Zhongguo Zhen Jiu. 2007;27(3):199–202.
8. Chen RX, Kang MF, He WL, et al. Moxibustion on heat-sensitive acupoints for treatment of myofascial pain syndrome: a multi-central randomized controlled trial. Zhongguo Zhen Jiu. 2008;28(6):395–8.

9. Chen RX, Kang MF, et al. Clinical application of acupoint heat-sensitization. Zhongguo Zhen Jiu. 2007;27(3):199–202.
10. Lin YF, Lu JM, Su YN, et al. Clinical Trials for Treatment of Allergic Rhinitis with Heat Sensitive Moxibustion and Its Regularity of Heat-sensitization Acupoint Distribution. Zhen Ci Yan Jiu. 2017;42(6):527–32.
11. He L, Jiang GP, Liu H, et al. Effects of acupoint heat-sensitization moxibustion on the gastrin and motilin in chronic diarrhea patients of Pi-Shen deficiency syndrome. Zhongguo Zhong Xi Yi Jie He Za Zhi. 2012;32(4):460–3.
12. Kim DH, Ryu Y, Hahm DH, et al. Acupuncture points can be identified as cutaneous neurogenic inflammatory spots. Sci Rep. 2017;7(1):15214.
13. Cheng B, Shi H, Ji CF, et al. Distribution of the activated acupoints after acute gastric mucosal injury in the rat. Zhen Ci Yan Jiu. 2010;35(3):193–7.
14. Shi H, Cheng B, Li JH, et al. Mast cell and substance P are involved in the process of acupoint sensitization induced by acute gastric mucosal injury. Zhen Ci Yan Jiu. 2010;35(5):323–9.
15. Lin J, Huang H, Ding GH, Zhang D. Relationship between the function of mast cells and acupuncture analgesia in adjuvant arthritis rats. Zhen Ci Yan Jiu. 2007;32(1):16–9.
16. Yao W, Yang HW, Yin N, Ding GH. Mast cell-nerve cell interaction at acupoint: modeling mechanotransduction pathway induced by acupuncture. Int J Biol Sci. 2014;10(5):511–9.
17. Zhang D, et al. Role of mast cells in acupuncture effect: a pilot study. Explore (NY). 2008;4(3):170–7.
18. Li L, Ding GH, Shen XY, et al. miR-199a-3p targets ETNK1 to promote invasion and migration in gastric cancer cells and is associated with poor prognosis. Pathol Res Pract. 2019;215(9):152511.
19. Wang JY, Li H, Ma CM, et al. Acupuncture may exert its therapeutic effect through microRNA-339/Sirt2/NFκB/FOXO1 axis. Biomed Res Int. 2015;2015:249013.
20. Zheng SP, Han W, Chu HR, et al. Effect of electroacupuncture and moxibustion pretreatment on expression of cerebral micro- RNAs and Aquaporin protein-4 in cerebral infarction rats. Zhen Ci Yan Jiu. 2015;40(2):99–103.
21. Bai FH, Ma YY, Guo HY, et al. Spinal Cord Glycine Transporter 2 Mediates Bilateral ST35 Acupoints Sensitization in Rats with Knee Osteoarthritis. Evid Based Complement Alternat Med. 2019;2019:7493286.
22. Li Y, Wu F, Wei J, Lao L, Shen X. The Effects of Laser Moxibustion on Knee Osteoarthritis Pain in Rats. Photobiomodul Photomed Laser Surg. 2020;38(1):43–50.
23. Kelly S, Dunham JP, Murray F, Read S, Donaldson L F,Lawsonet SN. Spontaneous firing in C-fibers and increased mechanical sensitivity in A-fibers of knee joint-associated mechanoreceptive primary afferent neurones during MIA-induced osteoarthritis in the rat. Osteoarthritis Cartilage. 2012;20(4):305–13.
24. Siiskonen H, Scheffel J. Isolation and Culture of Human Skin Mast Cells. Methods Mol Biol. 2020;2154:33–43.

25. Song Y, Zhang C, Zhang JX, et al. Localized injection of miRNA-21-enriched extracellular vesicles effectively restores cardiac function after myocardial infarction. Theranostics. 2019;9(8):2346–60.
26. Rivera J, Olivera A, Olivera. A current understanding of Fc epsilon RI-dependent mast cell activation. Curr Allergy Asthma Rep. 2008;8(1):14–20.
27. Kambayashi T, Koretzky GA. Proximal signaling events in Fc epsilon RI-mediated mast cell activation. J Allergy Clin Immunol. 2007;119(3):544–52. quiz 553-4.
28. Mishima S, Kashiwakura JI, Toyoshima S, et al. Higher PGD(2) production by synovial mast cells from rheumatoid arthritis patients compared with osteoarthritis patients via miR-199a-3p/prostaglandin synthetase 2 axis. Sci Rep. 2021;11(1):5738.
29. Karatay S, Karatay S, Okur SC, Uzkeser H, Yildirim K, Akcay F. Effects of Acupuncture Treatment on Fibromyalgia Symptoms, Serotonin, and Substance P Levels: A Randomized Sham and Placebo-Controlled Clinical Trial. Pain Med. 2018;19(3):615–28.
30. Fan Y, Kim DH, Gwak YS, et al. The role of substance P in acupuncture signal transduction and effects. Brain Behav Immun. 2021;91:683–94.
31. Yip KH, Kolesnikoff N, Hauschild N, et al. The Nedd4-2/Ndfip1 axis is a negative regulator of IgE-mediated mast cell activation. Nat Commun. 2016;7:13198.
32. Li J, Li YX, Luo LJ, Ye J, et al. The effectiveness and safety of acupuncture for knee osteoarthritis: An overview of systematic reviews. Medicine. 2019;98(28):e16301.
33. Shi GX, Tu JF, Wang TQ, et al. Effect of Electro-Acupuncture (EA) and Manual Acupuncture (MA) on Markers of Inflammation in Knee Osteoarthritis. J Pain Res. 2020;13:2171–9.
34. Luo X, Hou XS, Tian ZY, Meng X, Li SM, Bai P. Randomized controlled clinical trial of acupuncture treatment for knee osteoarthritis in the early stage. Zhen Ci Yan Jiu. 2019;44(3):211–5.
35. Gri G, Frossi B, D'Inca F, et al. Mast cell: an emerging partner in immune interaction. Front Immunol. 2012;3:120.
36. Olivera A, Rivera J. Sphingolipids and the balancing of immune cell function: lessons from the mast cell. J Immunol. 2005;174(3):1153–8.
37. Kitamura Y, Yokoyama M, Sonoda T, Mori KJ. Different radiosensitivities of mast-cell precursors in the bone marrow and skin of mice. Radiat Res. 1983;93(1):147–56.
38. Meurer SK, Neß M, Weiskirchen S, et al. Isolation of Mature (Peritoneum-Derived) Mast Cells and Immature (Bone Marrow-Derived) Mast Cell Precursors from Mice. PLoS One. 2016;11(6):e0158104.
39. Dahlin JS, Hallgren J. Mast cell progenitors: origin, development and migration to tissues. Mol Immunol. 2015;63(1):9–17.
40. Feuser K, Thon KP, Bischoff SC, Lorentz A. Human intestinal mast cells are a potent source of multiple chemokines. Cytokine. 2012;8(2):178–85.
41. Mukai K, Tsai M, Saito H, Galli SJ. Mast cells as sources of cytokines, chemokines, and growth factors. Immunol Rev. 2018;282(1):121–50.
42. Metcalfe DD, Baram D, Mekori YA. Mast cells. Physiol Rev. 1997;77(4):1033–79.

43. da Silva EZ, Jamur MC, Oliver C. Mast cell function: a new vision of an old cell. J Histochem Cytochem. 2014;62(10):698–738.
44. Frieri M, Patel R, Celestin J. Mast cell tryptase: a review of its physiology and clinical significance. Anaesthesia. 2004;59(7):695–703.
45. Petrosino S, Schiano Moriello A, Verde R, et al. Palmitoylethanolamide counteracts substance P-induced mast cell activation in vitro by stimulating diacylglycerol lipase activity. J Neuroinflammation. 2019;16(1):274.
46. Levick SP, Brower GL, Janicki JS. Substance P-mediated cardiac mast cell activation: An in vitro study. Neuropeptides. 2019;74:52–9.
47. Zhan M, Zheng W, Jiang Q, et al. Upregulated expression of substance P (SP) and NK1R in eczema and SP-induced mast cell accumulation. Cell Biol Toxicol. 2017;33(4):389–405.
48. Zhu G, Pei L, Lin F, Yin H, et al. Exosomes from human-bone-marrow-derived mesenchymal stem cells protect against renal ischemia/reperfusion injury via transferring miR-199a-3p. J Cell Physiol. 2019;234(12):23736–49.
49. Zhang K, Shao CX, Zhu JD, et al. Exosomes function as nanoparticles to transfer miR-199a-3p to reverse chemoresistance to cisplatin in hepatocellular carcinoma. Biosci Rep. 2020;40(7).
50. Zhao JL, Tan B, Chen G, et al. Hypoxia-Induced Glioma-Derived Exosomal miRNA-199a-3p Promotes Ischemic Injury of Peritumoral Neurons by Inhibiting the mTOR Pathway. Oxid Med Cell Longev. 2020;2020:5609637.

Figures

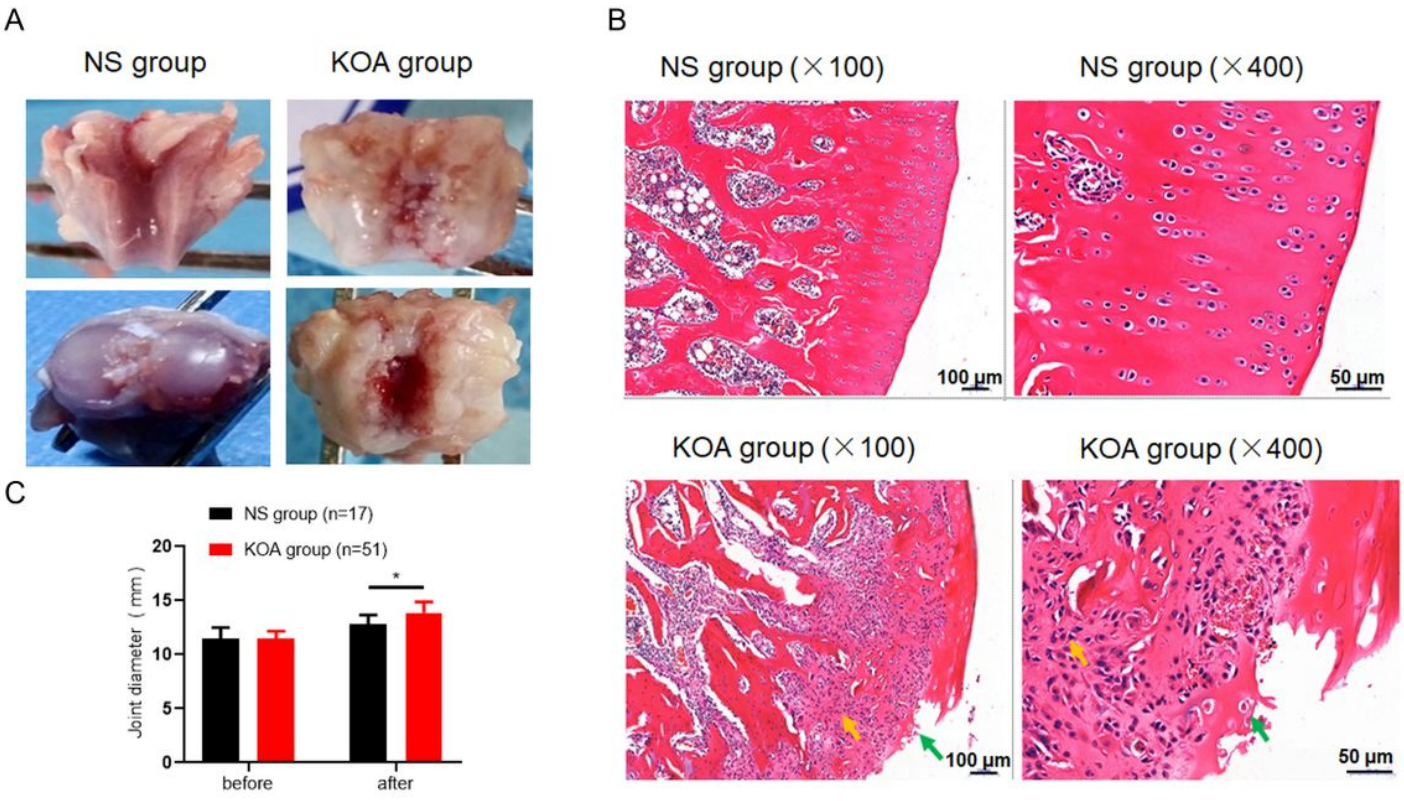

Figure 1

MIA induces KOA-related cartilage damage. A. Representative images of articular pathology at 14 days after saline (NS group) or MIA injection (KOA group). B. Representative images H&E-stained synovial tissues in the NS and KOA groups. Highlighted pathologies include fibrous hyperplasia (yellow arrows) and articular cartilage surface defects (green arrows). C. The diameter of left knee joint before and 14 days after treatment. *P < 0.05.

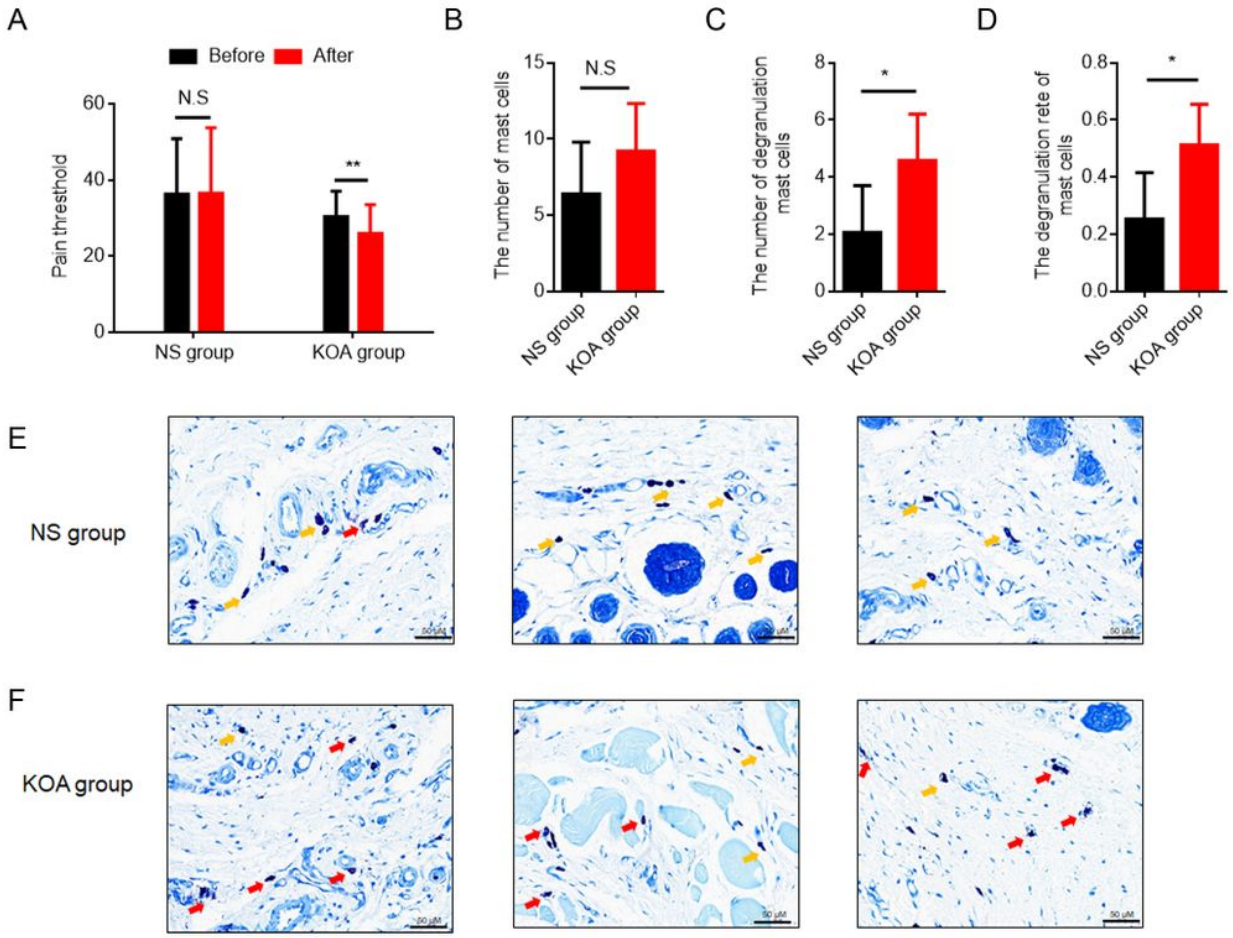

Figure 2

ST36 acupoints were sensitized after KOA modelling. A. The pain threshold in the NS or KOA group (n=12 each group). B. Number of mast cells in the NS or KOA groups (n=12 each group). C, D degranulation number (C) and degranulation rate (D) in the NS or KOA groups (n=12 each group). E, F. Representative ST36 skin sections showing mast cells stained with toluidine blue from the NS (E) and KOA groups (F). Highlighted areas show mast cells without degranulation (yellow arrows) and with degranulation (red arrows). *P < 0.05; **P < 0.01; NS, not significant.

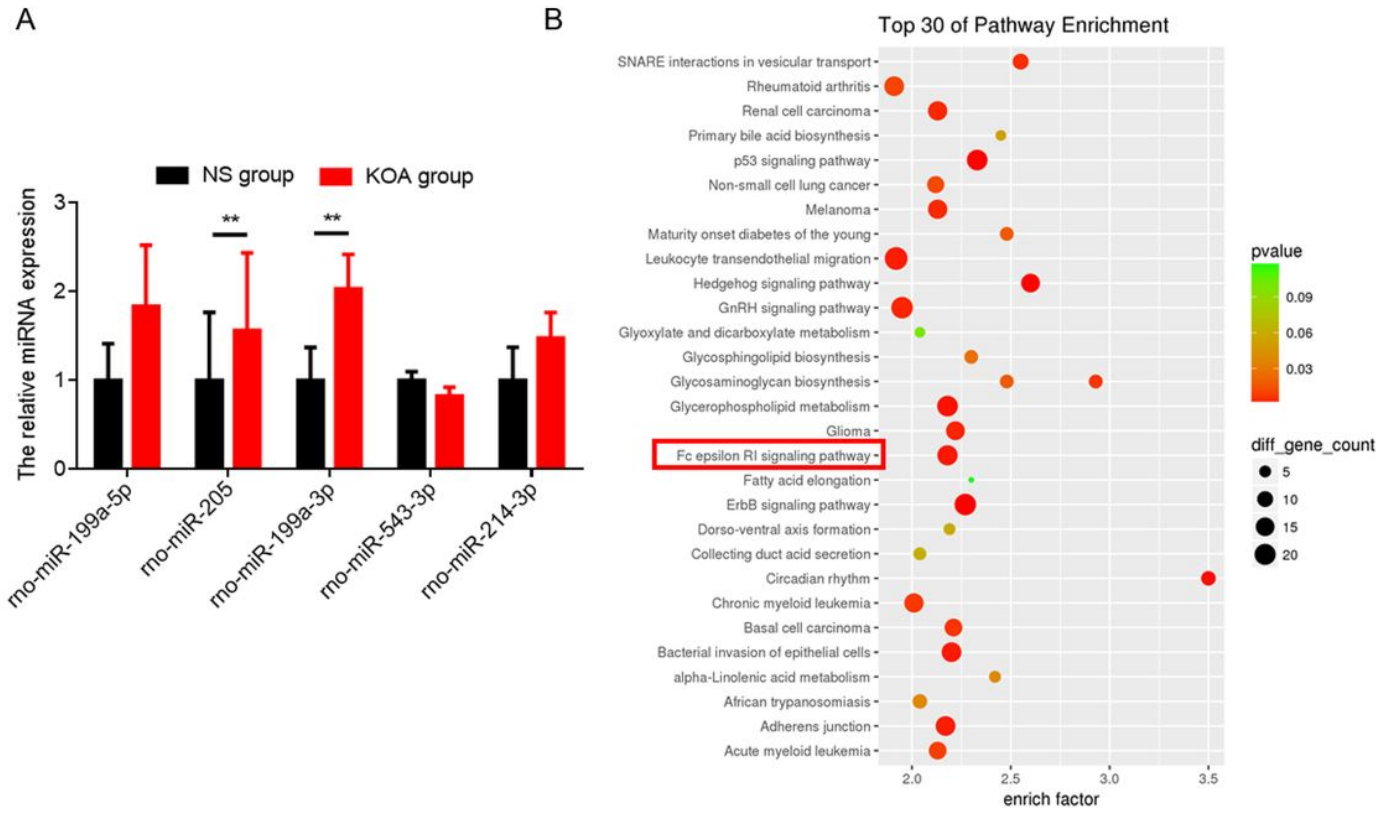

Figure 3

Differentially expressed miRNAs in the ST36 acupoint in KOA rats and their predicted pathway effects. A. RT-qPCR validation of five differentially expressed miRNAs determined from the RNA-seq analysis (n=6 each group). B. The top enriched KEGG signaling pathways predicted from genes targeted by the differentially expressed miRNAs. The red box highlights pathways related to mast cell activation. *P < 0.05; **P < 0.01.

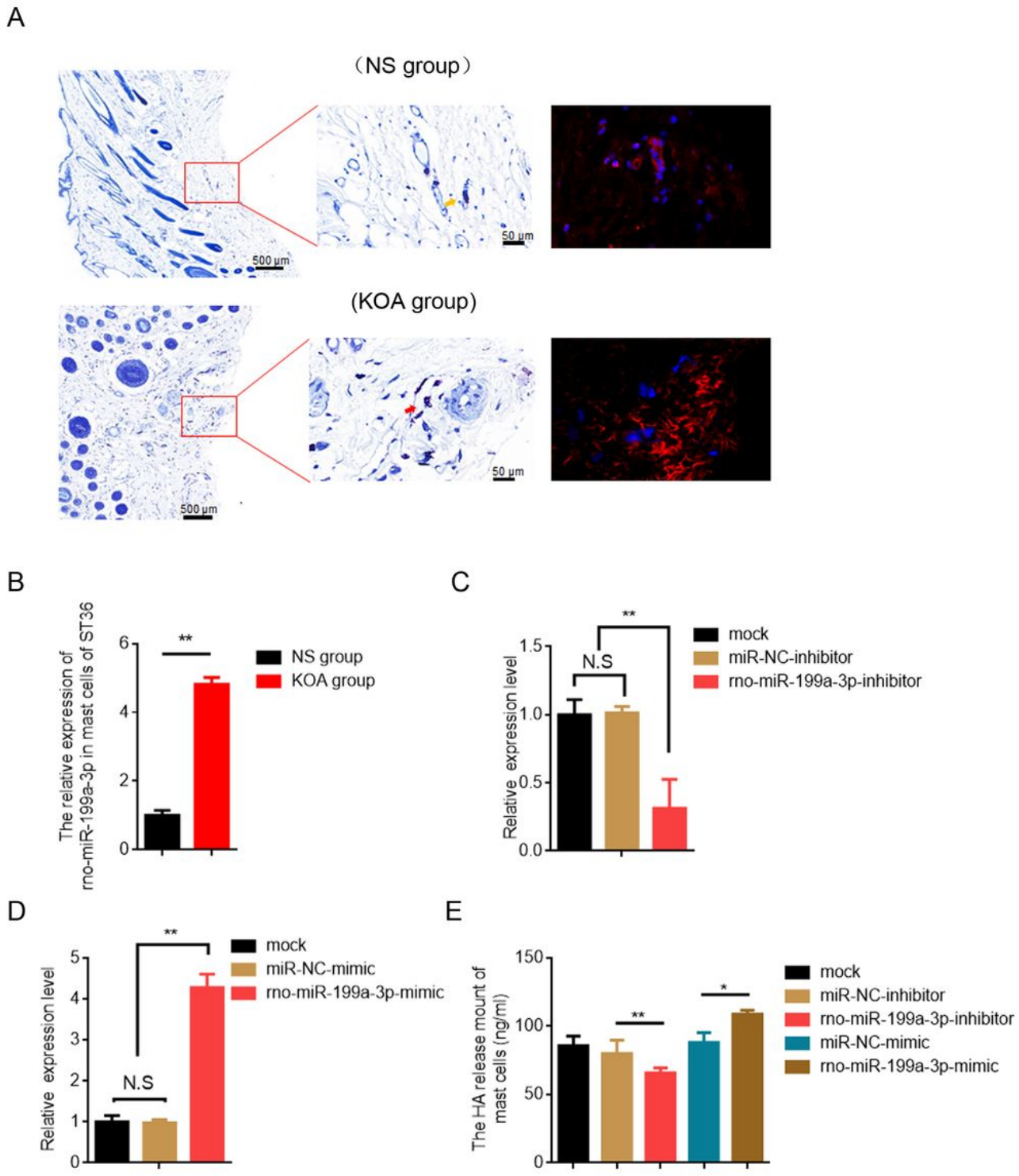

Figure 4

Mast cell activation is regulated through rno-miR-199a-3p. A. Mast cells in ST36 skin tissues stained with toluidine blue (left panels) are compared with FISH analysis of miR-199a-3p expression (red fluorescence; right panels). Nuclei were counterstained with DAPI (blue fluorescence). B. RT-qPCR analysis of rno-miR-199a-3p levels in skin mast cells isolated from the ST36 acupoint in NS and KOA group rats (n=3). C, D. RT-qPCR analysis of rno-miR-199a-3p levels in cultured mast cells transfected with mock, control NC or

rno-miR-199a-3p inhibitors (C) or mock, control NC or rno-miR-199a-3p mimics (D) (n=3). E. Histamine (HA) release in cultured mast cells transfected as indicated with miRNA-inhibitor or miRNA-mimics before stimulation with 50 μm SP for 30 min. *P < 0.05; **P < 0.01; NS, not significant

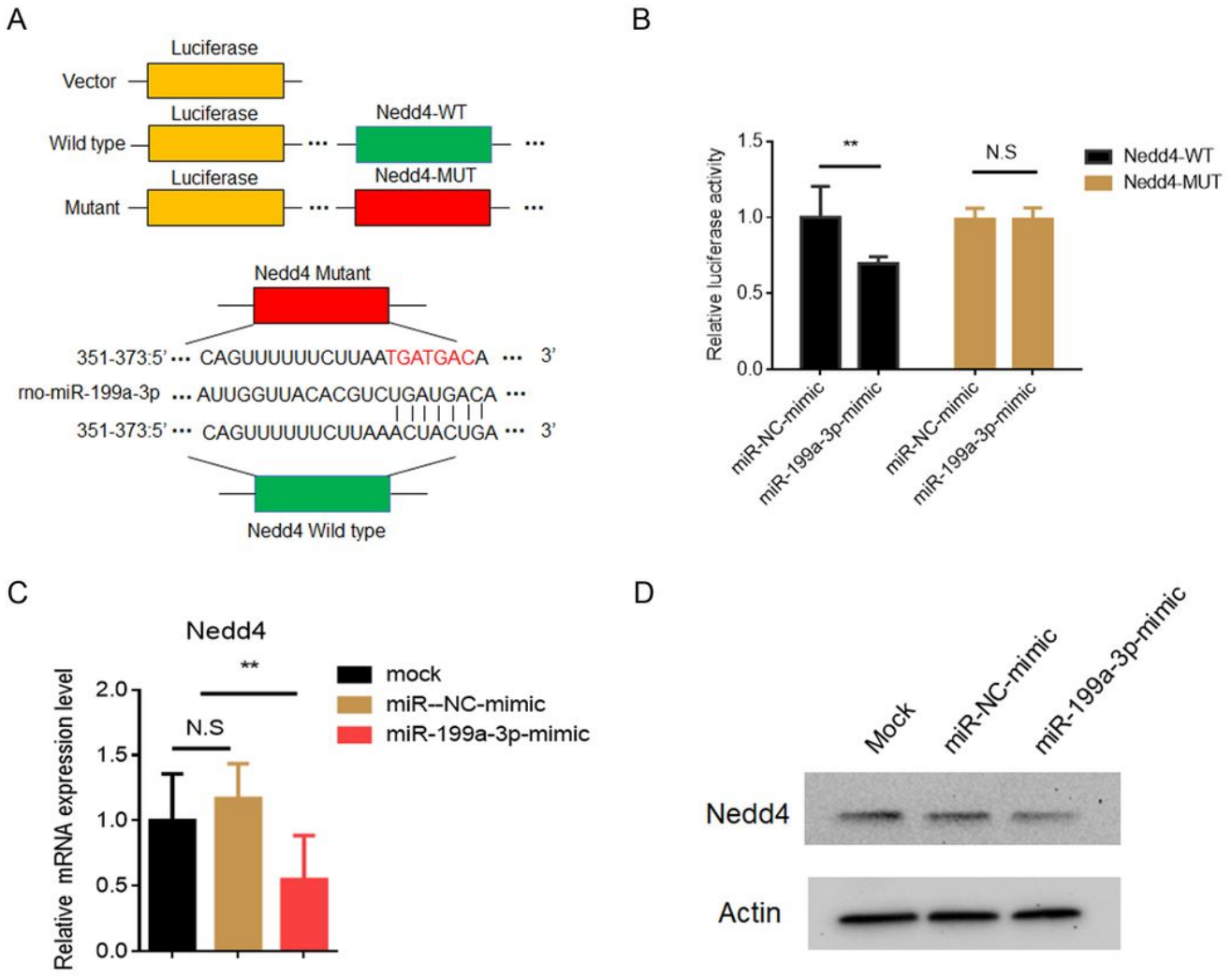

Figure 5

Rno-miR-199a-3p inhibits Nedd4 expression by targeting the 3' UTR region of Nedd4 mRNA. A. TargetScan database analysis identified a potential binding site for rno-miR-199a-3p in the Nedd4 3'-UTR. As illustrated, wild-type and mutant reporter constructs were prepared in the pmiR-GLO reporter vector. B. Luciferase reporter assay conducted in HEK-293 cells after transfection with the wild-type or mutant pmiR-GLO reporter constructs in combination with either rno-miR-199a-3p mimics or control NC mimics. C, D. Cultured mast cells were transfected with NC or rno-miR-199a-3p mimics and the levels of Nedd4 mRNA (C) and protein (D) determined using RT-qPCR and Western blotting, respectively. *P < 0.05; **P < 0.01; NS, not significant

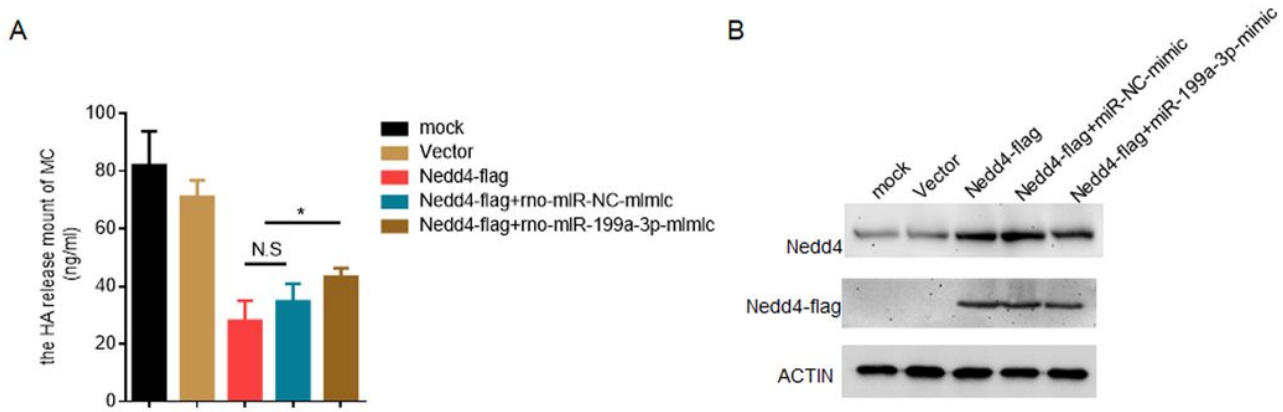

Figure 6

Rno-miR-199a-3p promotes mast cell activation via Nedd4. A. Histamine (HA) release in cultured mast cells transfected with Mock or control plasmids (Vector) or the indicated combinations of the Nedd4-flag overexpression plasmid and rno-miR-199a-3p mimics. B. Western blotting analysis against cells from (A) using antibodies directed against Nedd4, Flag or Actin. *P < 0.05; NS, not significant